Intracellular Metabolism, Subcellular Localization and Phototoxicity of HMME/HB in Ovarian Cancer Cells

KUN SONG[1*], JIE LI[1*], LI LI[1], PEIHAI ZHANG[1], FENG GENG[1], RUIFEN DONG[1], QIFENG YANG[2], XUN QU[3] and BEIHUA KONG[1]

Departments of [1]Obstetrics and Gynecology, [2]Breast Surgery and [3]Basic Medicine Institution, Qilu Hospital, Shandong University, Ji'nan, Shandong, P.R. China

Abstract. *Background: Photodynamic therapy (PDT) is considered a promising new strategy for ovarian cancer treatment. As the key component in PDT, photosensitizer metabolism and localization in cancer cells is particularly important. Materials and Methods: The localization of the photosensitizers hematoporphyrin monomethyl ether (HMME) and hypocrellin B (HB) were determined in the ovarian cancer cell lines SKOV3 and NuTu-19 by fluorescence microscopy and laser scanning confocal microscopy(LSCM). A JD801 image analysis system was used to analyze the fluorescence intensity of the photosensitizers in the cells. The phototoxicity of both drugs to the cancer cells was determined by MTT assay. Results: Both photosensitizers were mainly distributed in the cytoplasm. Drug uptake reached a peak after 4 h incubation with HB and after 3 h incubation with HMME. Within a certain range, the higher the concentration, the stronger the fluorescence became and at 40 μg/ml, the intracellular photosensitizer had reached saturation. Based on these results PDT was applied to SKOV3 cells. All the cells were killed when the photosensizer dose reached 40 μg/ml. Conclusion: PDT is an effective therapy for ovarian cancer cells.*

At present, the treatment for ovarian cancer includes three main strategies: surgery, chemotherapy and radiotherapy (1-3). Although considerable progress in these areas has been attained, most patients with advanced stage ovarian cancer experience recurrence and eventually die of their disease. It is estimated that 130,000 deaths per year occur from ovarian cancer worldwide (4). Therefore, more effective and safe alternative treatments, such as photodynamic therapy (PDT), are needed.

PDT involves the uptake of a photosensitizer by the tumor tissue, followed by illumination of the tumor tissue by visible light of a specific wavelength to generate cytotoxic molecules such as singlet oxygen and other oxygen species, which leads to the apoptosis or necrosis of the cancer cells (5-8). PDT is considered a promising new strategy for ovarian cancer due to its dual selectivity produced by both the preferential uptake of a photosensitzer by cancer cells and restriction of the illumination localization to confine activation of the photosensitizer (9). The photosensitizer is the key component in PDT, and its localization within cancer cells is particularly important for research into photodamage to cells. Investigations of the intracellular localization and quantitative analysis of the fluorescence intensity in cells are also essential for determination of the mechanisms of cell death by photosensitizers, and can provide a basis for the use of PDT in the treatment of ovarian cancer (10, 11). Several clinical trials showed positive effects of PDT using first-generation photosensitizer dihematoporphyrin ether and porfimer sodium in treating peritoneal malignancy including ovarian cancer (12, 13). However, the toxicity of the first-generation photosensitizer was notable. More research of PDT using new types of photosensitizers is necessary.

HB, metabolites of which are present in the parasitic fungus *Hypocrella bambusae* that is abundantly grown in Yunnan Province of China, is the second generation of photosensitizer developed independently by China (14, 15). Another photosensitizer, HMME, that developed in China is now produced commercially. Although the application of HB and HMME in vulvar white lesions and port wine stains has achieved good effects (16, 17), their application in the treatment of cancer has been rarely reported (18, 19). Both HB and HMME can lead to cell death by apoptosis or necrosis depending on concentration, laser irradiation dose,

*Both authors ontributed equally to this work.

Correspondence to: Beihua Kong, MD, Ph.D., Department of Obstetrics and Gynecology, Qilu Hospital of Shandong University, Ji'nan 250012, Shandong Province, P.R. China. Tel: +86 53182169008. Fax: +86 53186927544, e-mail: kongbeihua@yahoo.com.cn; songkun2001226@yahoo.com.cn

Key Words: Ovarian cancer, hyprocrellin B, hematoporphyrin monomethyl ether, intracellular metabolism, subcellular localization, phototoxicity.

illumination time, tumor cell type and intracellular localization (20-23).

In this study, the localization of HMME and HB was determined in the human ovarian epithelial cancer cell line SKOV3 and the rat ovarian epithelial cancer cell line NuTu-19 by inverted fluorescence microscopy equipped with cooled intensified charge coupled device (ICCD) and laser scanning confocal microscopy (LSCM).

Materials and Methods

Materials. HMME was purchased from Shanghai FuDan-ZhangJiang BioPharmaceutical (Shanghai, China) and HB was purchased from Institute of Biophysics, Chinese Academy of Sciences (Beijing, China). RPMI 1640 culture medium, high glucose DMEM culture medium and new fetal bovine serum were purchased from Invitrogen Gibco (Shanghai, China). Dimethyl sulfoxide (DMSO) was obtained from Sigma China (Beijing, China). The Olympus IX81 inverted fluorescence microscope and Olympus Fluoview FV500 laser scanning confocal microscope LSCM were purchased from Olympus (Olympus, Tokyo, Japan).

Cell lines and cell culture. The human ovarian epithelial cancer cell line SKOV3 and the rat epithelial ovarian cancer cell line NuTu-19 were obtained from the Basic Medicine Research Institute, Qilu Hospital, Shandong University, PR China. The SKOV3 and NuTu-19 cells were cultured in RPMI 1640 medium and DMEM medium enriched with 10% fetal bovine serum, respectively. Both of the cell lines were incubated under standardized conditions (37˚C, 5% carbon dioxide, 100% humidity). When the cells were in the logarithmic growth phase, they were digested with 0.25% trypsin and 0.02% EDTA for subsequent assays.

Preparation of HB and HMME solutions. The HB solution was prepared fresh prior to use by dissolving HB in DMSO at a concentration of 2 mg/ml. The HMME solution was prepared similarly, except the solvent was DMEM. Both solutions were kept in the dark at 4˚C. Further dilutions of HB and HMME were performed in serum-free media to obtain the different concentrations used.

Images of the photosensitizer in cells by inverted fluorescence microscopy. The SKOV3 cells (10^4/ml) were seeded into 12-well plates, and after 24 h incubation, the medium was refreshed with serum-free medium containing 40 μg/ml photosensitizer. After incubation for various time intervals (1.5 h, 2.5 h, 3.5 h, 4.5 h and 5.5 h) at 37˚C with light protection, the plates were washed three times with phosphate-buffered saline (PBS) and new serum-free medium was added. Fluorescent images were acquired with an Olympus IX81 inverted fluorescence microscopic equipped with a cooled ICCD. Three different light sources were selected, including ultraviolet light (U1), blue light (B1) and green light (G1); the exciting wavelengths were, respectively, 330-380 nm, 450-480 nm and 510-550 nm, and the emitting wavelengths were, respectively, >420 nm, >515 nm and >590 nm. Exposure time was 1/60 second. The images captured by the cooled ICCD camera were processed using Image-Pro software (MediaCybernetics, Bethesda, MD, USA), and saved in TIF (Tagged Image File Format) format. The images at different time intervals were captured using the same instrument and the same software parameters to avoid differences caused by the device.

The SKOV3 cells were also incubated with different concentrations of the photosensitizers (10 μg/ml, 20 μg/ml, 40 μg/ml, 60 μg/ml or 80 μg/ml) for 3 h, and then images were captured by inverted fluorescence microscopy. The same experiment was also done on the NuTu-19 cells in the same way as for the SKOV3 cells.

LSCM images of the photosensitizer in cells. Sterile quartz coverslips were placed into 24-well plates, and the SKOV3 or NuTu-19 cells (10^4/ml) were seeded onto the coverslips. After 24 h incubation, the medium was refreshed with serum-free culture media containing the photosensitizer HB or HMME at a concentration of 40 μg/ml. Following incubation for 3 h, images were captured by Olympus FV500 LSCM (Olympus, Tokyo, Japan). During the process of capture, serum-free medium was continuously added to ensure normal morphology of the cells. Two types of excitation waves were used: a 488 nm wave generated by a multi-line argonion laser for HMME and a 543 nm wave generated by a helium-neon laser for HB. The emitting wave length of the LSCM were both >560 nm. Different forms of the images were acquired including the common light differential interference contrast (DIC) form, the laser exciting fluorescence form, and a combination of the above two forms, which were then analyzed.

Fluorescence intensity analysis. Images captured by by inverted fluorescence microscopy after various incubation time intervals and with various drug concentrations were analyzed by the JD801 image analysis system (JEDA Science-Technology Development Company, JiangSu Province, PR China). Briefly, the images were analyzed by various methods including the color image segmenting method, the hole filling method, the border smoothing method and the granule deleting method to select the fluorescence region in the cells. The fluorescence intensity of the photosensitizer in the cells is presented as the average optical density.

Photodynamic treatment of the cells. The SKOV3 cells line was choosen for phototoxicity experiments *in vitro*. The cells in 200 μl of 10% FCS RPMI 1640 medium (1.5×10^4 cells/well) were seeded in 96-well flat-bottomed microtiter plates and incubated for 24 h at 37˚C in a 5% CO_2 incubator. When the cells were in the exponential growth phase, the supernatants were removed and replaced with 200 μl fresh FCS-free medium containing the photosensitizer HMME or HB. The cells were incubated with varying concentrations of HMME (0~40 μg/ml) for 3 h or with HB (0~40 μg/ml) for 4 h. The medium containing the drug was then aspirated and the cells were rinsed with PBS followed by replacement with another 200 μl RPMI 1640 before laser illumination. The laser source was a pulsed dye laser (Quantel Datachrom 5000, Quantel, Clermont-Ferrand, Frence) operating at a frequency of 10 Hz. Irradiation was carried out with various light dose (0~6 J/cm^2) at 620 nm with an output of 160 mw. Following this treatment, the medium was replaced by 10% FCS RPMI 1640 and the cells were grown on again for a further 24 h. To evaluate cell viability and calculate the percentage of phototoxicity, the MTT assay was employed.

Phototoxicity assay. Photosensitizer-mediated cytotoxicity was determined by the tetrazolium chlorimetric reduction assay [3-(4,5-dimethylthiazol-2-yl)-2,5-diphenyltetrazolium bromide, MTT assay], which measures the mitochondrial dehydrogenase activity of surviving cells, as described previously (24, 25). Briefly, the wells containing media without photosensitizer treatment served as positive control and 200 μl of the medium alone without cells or reagents was

used as negative control. Following the photodynamic treatment and additional 24 h incubation of the cells in the 96-well plate, 20 μl of the MTT dye (5 mg/ml) were added into each well and the plate was incubated for an additional 4 h. The unreactive supernatants in the well were carefully aspirated and replaced with 100 μl of DMSO to dissolve the reactive dye. The absorbance (A) values of each well at 490 nm were read using an automatic multiwell spectrophotometer (Bio-Rad-Coda, Richmond, CA, USA). The negative control well was used for zeroing absorbance. The percentage of survival was calculated using the background-corrected absorbance as follows:
Survival rate=*A* of experimental well/*A* of positive control well ×100%
The experiments were performed at least 3 times with representative data presented.

Statistical analysis. The statistical analysis was performed using SPSS software (SPSS Inc., Chicago, IL, USA), and the differences between groups were analyzed by Student's *t*-test. A value of $p<0.05$ was regarded as indicating statistical significance.

Results

Images of HB and HMME in cells by inverted fluorescence microscopy. Using inverted fluorescence microscopy, after incubation with 40 μg/ml of HB, red fluorescence in the cells was identified by excitation with B1 and G1 beams; however, no fluorescence was seen with U1 beam excitation. For the photosensitizer HMME, red fluorescence was identified in cells by excitation with all three beams (Figures 1 and 2). Following the various time interval and concentration incubations, both of the photosensitizers were mainly distributed in the cytoplasm of the NuTu-19 and SKOV3 cells, and there was little or no distribution in the nucleus of the cells.

Images by laser confocal microscopy. The distributions of photosensitizers in the ovarian cancer cells determined by LSCM was similar to that by inverted fluorescence microscopy. The red fluorescence was more distinct in the images obtained with confocal microscopy than in those obtained with fluorescence microscopy and the dye appeared to be distributed widely throughout the cytoplasm in a punctuate pattern (Figures 1 and 2).

Analysis of intracellular fluorescence intensity. The intracellular fluorescence intensities after different incubation intervals and with different photosensitizer concentrations are shown in Figures 3 and 4. Optical density reached a peak after 4 h incubation with HB and after 3 h incubation with HMME, and subsequently decreased along with time. Within the range of concentration used, the higher the concentration, the stronger the fluorescence became and statistical differences in the fluorescence intensity were found between different photosensitizer concentration groups ($p<0.05$). When the photosensitizer concentration reached 40 μg/ml, no additional effect on fluorescence intensity with increasing photosensitizer concentration was demonstrated, indicating that the intracellular photosensitizer had reached saturation.

Phototoxicity effect in vitro. Based on the above study results, 40 μg/ml was choosen as the maximum dose in the phototoxicity assay. The MTT assay showed no significant difference in the survival rate of the cells exposed to light alone ($p>0.05$) or drug alone ($p>0.05$) compared to blank controls (cells that received neither light nor drug). When the photosensitizers were combined with laser illumination, the photocytotoxicity was both drug dose- and light dose-dependent. The survival rate of the cells was significantly decreased with increasing light doses (2~6 J/cm^2, $p=0.004$) and similarly in cells receiving increasing photosensitizer doses (0~40 μg/ml, $p=0.001$). The SKOV3 cells were very sensitive to HB/HMME based photodynamic treatment. Though intracellular photosensitizer saturation was reached by 40 μg/ml, all the cells could be killed with an even lower drug dose (10 μg/ml), as shown in Figure 5.

Discussion

Although many instruments, such as fluorescence microscopy and confocal microscopy, have both been used for the determination of the fluorescence emitted by photosensitizers after light excitation in cells. However the fluorescence receiving and transmitting device for simple microscopy is a CCD (Charge Coupled Device), which cannot detect the weak fluorescence of a photosensitizer due to its low sensitivity. Confocal microscopy is more sensitive to weak fluorescence, but is expensive, consequently the cost of performing assays is higher compared to those using simple fluorescence microscopy. Therefore, the development of an easy, inexpensive and highly sensitive method for the measurement of fluorescence is necessary.

ICCD can capture extremely weak fluorescence, since it has a cooling system, which overcomes electronic thermal noise and greatly decreases non-specific background noise and its microchannel plate image intensifier enhances the optical sensitivity and optical amplification of the ICCD, needing, thus, only one capture to obtain a distinct image. Therefore, it doesn't only detect the weak fluorescence, but also significantly reduces the fluorescence excitation time and excitation number, avoiding, thus, photo-bleaching and minimizing photodamage to cells. The photosensitizers HB and HMME are easy to quench, but in the present study distinct fluorescence was identified even at an extremely low concentration (10 μg/ml) using an ICCD. As seen in this study, HB and HMME emitted red fluorescence with excitation by blue and green light, but no fluorescence was identified for HB with ultraviolet because a non-absorption peak existed in the wavelength of 300~400 nm. Both HB and HMME were mainly distributed in the cytoplasm of the NuTu-19 and SKOV3 cells, and there was little or no distribution in the nucleus. The photosensitizers were distributed widely throughout the cytoplasm in a punctuate

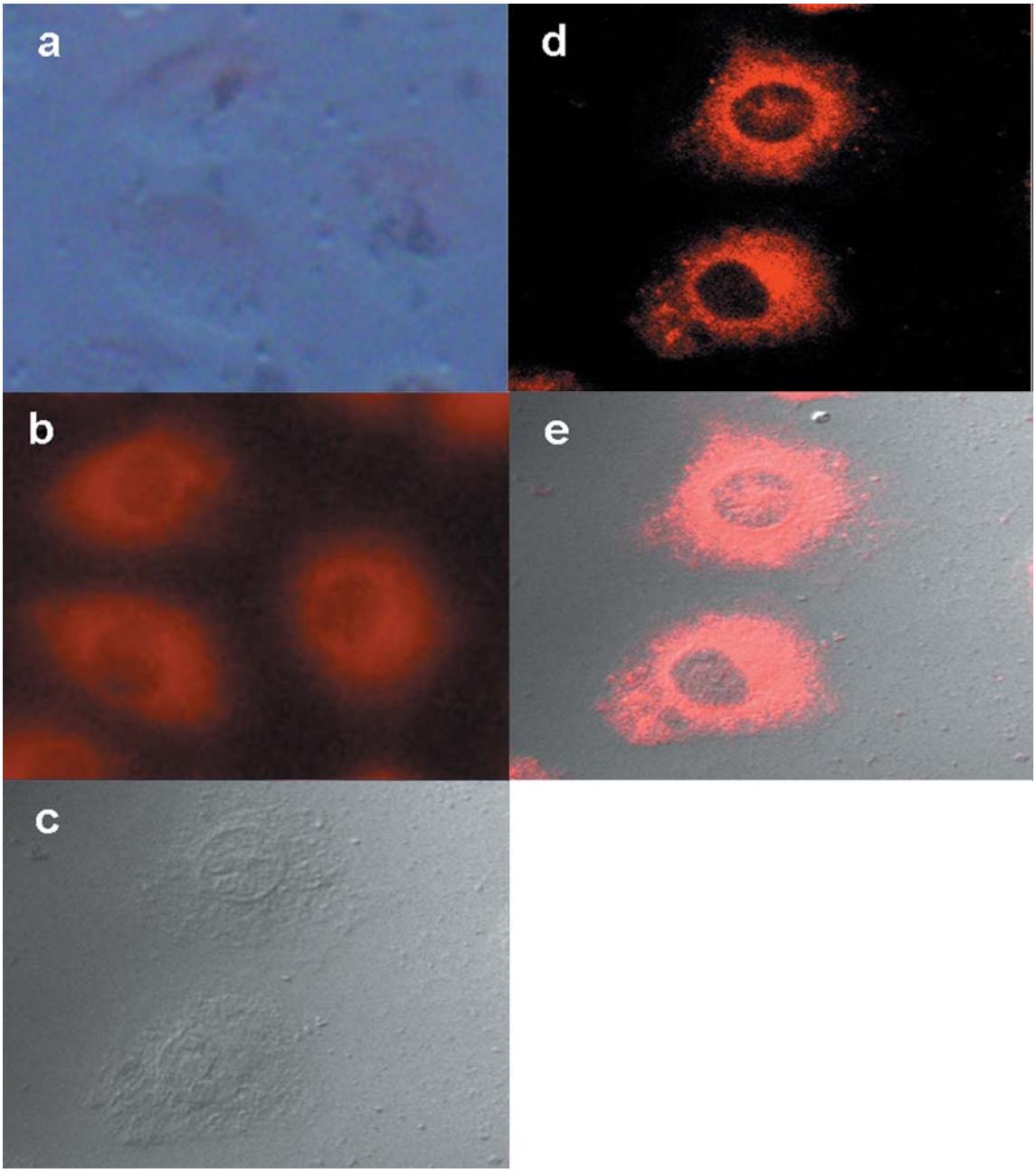

Figure 1. *Fluorescence images of HMME/HB in NuTu-19 cells. Ordinary light (a); Fluorescence microscope (b); Differential Interference contrast (DIC) (c); Laser confocal scanning microscopy (LCSM) image (d); Superimposition of (c) and (d) (e).*

pattern and the fluorescence intensity was not uniform indicating that the photosensitizers might be localized in the mitochondria, lysosomes, golgi apparatus and endoplasmic reticulum.

LSCM has been extensively used for the investigation of intracellular localization and photodamage target sites of photosensitizers. In the present study LSCM was used to further identify the localization of the photosensitzers in the cells and the results were similar to those with fluorescence microscopy equipped with ICCD. In addition, the use of fluorescence microscopy with an ICCD in conjunction with the JD801 image analysis system to determine the intracellular fluorescence intensity achieved good results and provided a lower cost, less complicated alternative to LSCM.

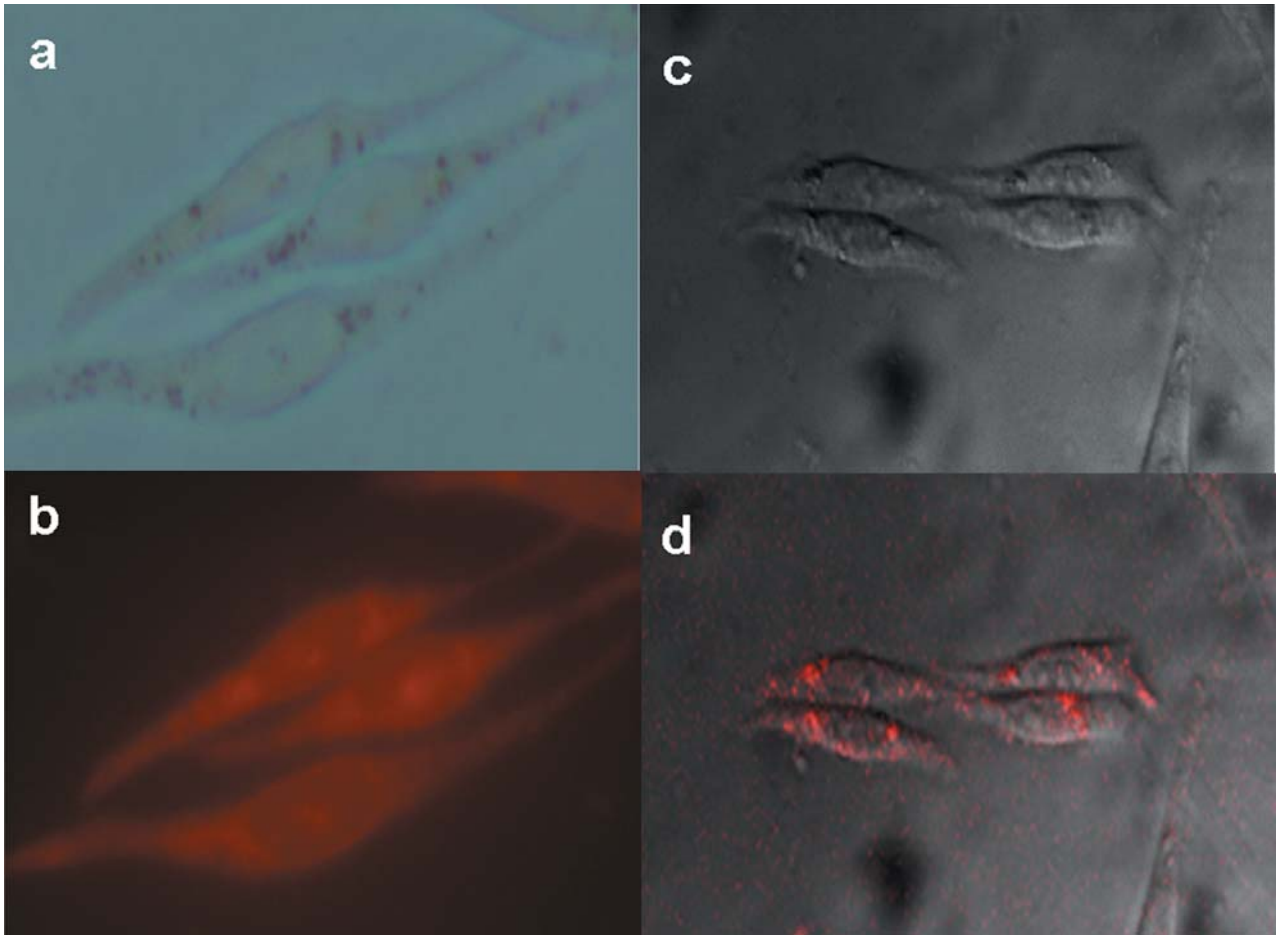

Figure 2. *Fluorescence images of HMME/HB in SKOV3 cells. Ordinary light (a); Fluorescence microscope (b); Differential Interference contrast (DIC) (c); Laser confocal scanning microscopy (LCSM) (d).*

The fluorescence intensity reached a peak after 4 h incubation for HB and after 3 h incubation for HMME and these optimal exposure times were selected in order to achieve the best therapeutic effects. The intracellular fluorescence intensity increased until the photosensitizer concentration reached 40 μg/ml, indicating that there was a maximum absorption value in the cells. Phototoxicity was clearly demonstrated as all the SKOV3 cells were killed when photosensizer dose reached 40 μg/ml.

Conclusion

In summary, the combined application of a fluorescence microscopy equipped with ICCD and an image analysis system is a potential method for investigating the localization and quantitative analysis of fluorescence intensity in cells. The images obtained with this easy, inexpensive and highly sensitive method were similar to those with LSCM and

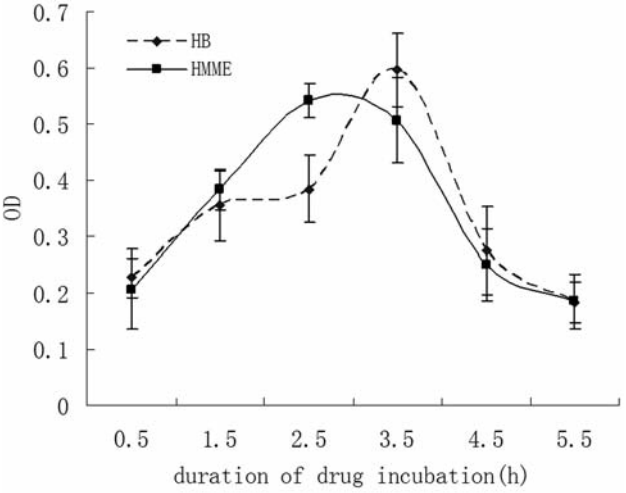

Figure 3. *Time-fluorescence intensity curve of HB and HMME (40 μg/ml) in SKOV3 cells.*

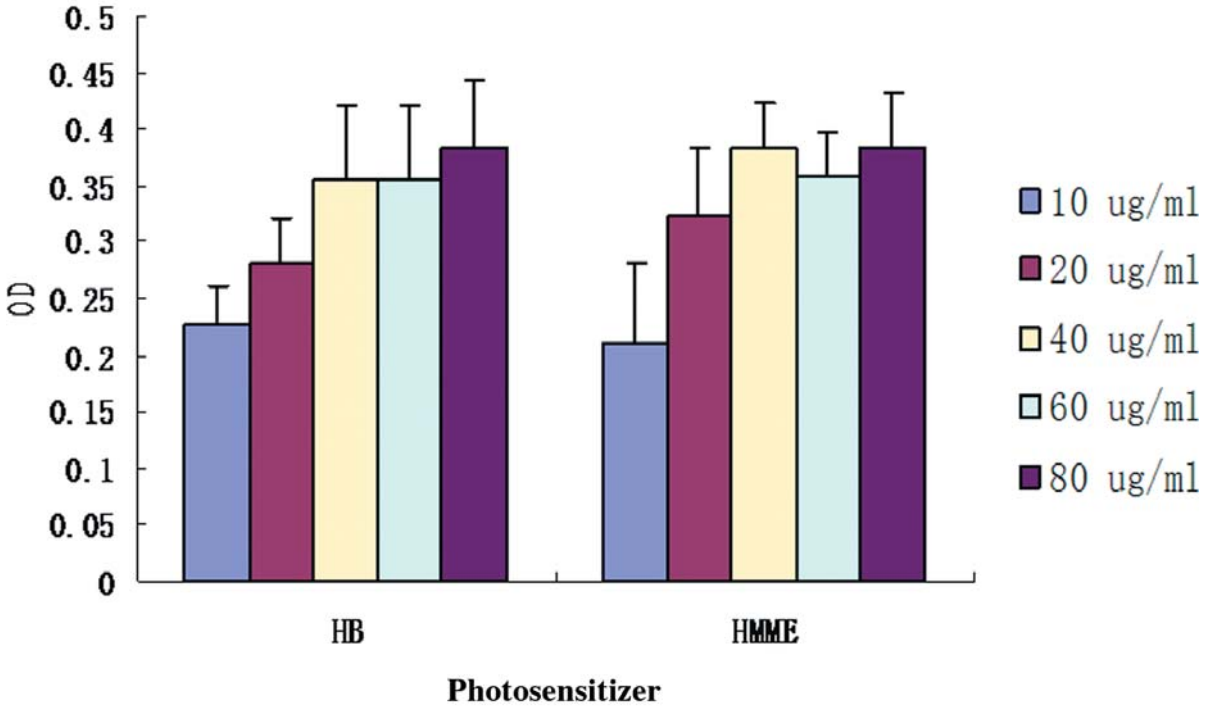

Figure 4. *Fluorescence intensity of different concerntrations of HB and HMME in SKOV3 cells.*

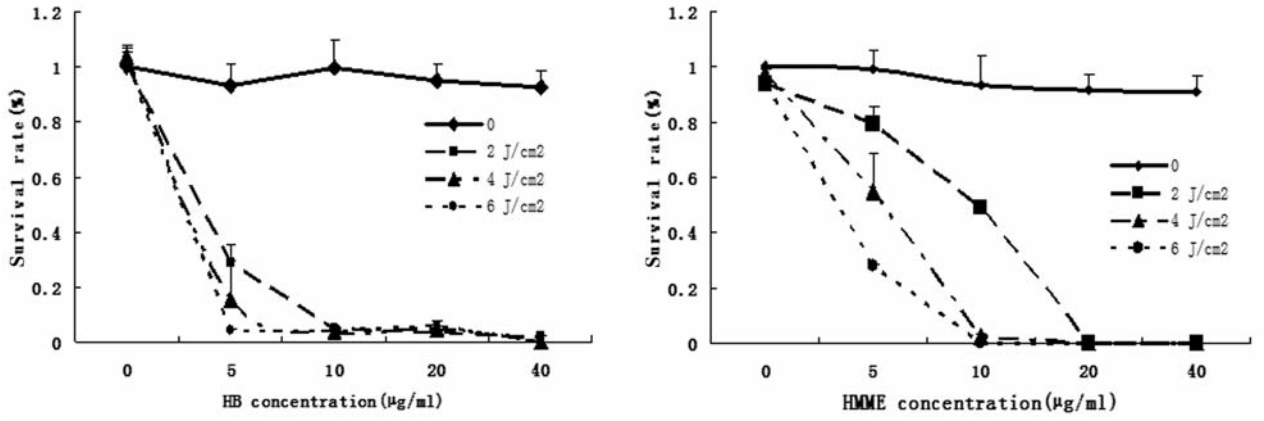

Figure 5. *Photocytotoxity of HB and HMME in SKOV3 cells. Shown are the cell survival rates 24 h after photodynamic treatment with different concentrations of drugs (0~40 μg/ml) and different light doses (0~6 J/cm^2).*

demonstrated clearly the intracellular metabolism and subcellular location of HMME and HB in the ovarian cancer cells. The photosensitizers HB and HMME were mainly distributed in the cytoplasm of the cells and the optimal incubation time and photosensitizer concentration were demostrated. Using these parameters, maximum phototoxicity was achieved. In conclusion, PDT is an effective therapy in ovarian cancer cells.

Disclosures

The authors have no conflicts of interest to disclose.

Acknowledgements

This work was supported by grants from National Natural Science Foundation of China (No. 30700897) and Doctor Foundation of Education Ministry (20090131120063) to Kun Song.

References

1 Guarneri V, Piacentini F, Barbieri E and Conte PF: Achievements and unmet needs in the management of advanced ovarian cancer. Gynecol Oncol *117*: 152-158, 2010.

2 Bookman MA: Standard treatment in advanced ovarian cancer in 2005: the state of the art. Int J Gynecol Cancer *15*: 212-220, 2005.

3 Ozols RF: Treatment goals in ovarian cancer. Int J Gynecol Cancer *15*: 3-11, 2005.

4 Wakui M, Yokoyama Y, Wang H, Shigeto T, Futagami M and Mizunuma H: Efficacy of a methylester of 5-aminolevulinic acid in photodynamic therapy for ovarian cancers. J Cancer Res Clin Oncol *136*: 1143-1150, 2010.

5 Triesscheijn M, Baas P, Schellens JH and Stewart FA: Photodynamic therapy in oncology. Oncologist *11*: 1034-1044, 2006.

6 Almeida RD, Manadas BJ, Carvalho AP and Duarte CB: Intracellular signaling mechanisms in photodynamic therapy. Biochim Biophys Acta *1704*: 59-86, 2004.

7 Agostinis P, Buytaert E, Breyssens H and Hendrickx N: Regulatory pathways in photodynamic therapy induced apoptosis. Photochem Photobiol Sci *3*: 721-729, 2004.

8 Buytaert E, Dewaele M and Agostinis P: Molecular effectors of multiple cell death pathways initiated by photodynamic therapy. Biochim Biophys Acta *1776*: 86-107, 2007.

9 Dima VF, Vasiliu V and Dima SV: Photodynamic therapy: an update. Roum Arch Microbiol Immunol *57*: 207-230, 1998.

10 Oleinick NL and Evans HH: The photobiology of photodynamic therapy: cellular targets and mechanisms. Radiat Res *150*: S146-156, 1998.

11 Peng Q, Moan J and Nesland JM: Correlation of subcellular and intratumoral photosensitizer localization with ultrastructural features after photodynamic therapy. Ultrastruct Pathol *20*: 109-129, 1996.

12 Hendren SK, Hahn SM, Spitz FR, Bauer TW, Rubin SC, Zhu T, Glatstein E and Fraker DL: Phase II trial of debulking surgery and photodynamic therapy for disseminated intraperitoneal tumors. Ann Surg Oncol *8*: 65-71, 2000.

13 Hahn SM, Fraker DL, Mick R, Metz J, Busch TM, Smith D, Zhu T, Rodriguez C, Dimofte A, Spitz F, Putt M, Rubin SC, Menon C, Wang HW, Shin D, Yodh A and Glatstein E: A phase II trial of intraperitoneal photodynamic therapy for patients with peritoneal carcinomatosis and sarcomatosis. Clin Cancer Res *12*: 2517-2525, 2006.

14 Nenghui W and Zhiyi Z: Relationship between photosensitizing activities and chemical structure of hypocrellin A and B. J Photochem Photobiol B *14*: 207-217, 1992.

15 Diwu Z, Zhang C and Lown JW: Photosensitization with anticancer agents. 18. Perylenequinonoid pigments as potential photodynamic therapeutic agents: preparation and photodynamic properties of amino-substituted hypocrellin derivatives. Anticancer Drug Des *8*: 129-143, 1993.

16 Yuan KH, Li Q, Yu WL, Zeng D, Zhang C and Huang Z: Comparison of photodynamic therapy and pulsed dye laser in patients with port wine stain birthmarks: a retrospective analysis. Photodiagnosis Photodyn Ther *5*: 50-57, 2008.

17 Gu Y, Huang NY, Liang J, Pan YM andLiu FG: Clinical study of 1949 cases of port wine stains treated with vascular photodynamic therapy (Gu's PDT). Ann Dermatol Venereol *134*: 241-244, 2007.

18 Wang JB, Liu LX, Pan SH, Wang CY and Fu QF: Therapeutic effect of photodynamic therapy using hematoporphyrin monomethyl ether (HMME) on human cholangiocarcinoma cell line QBC939. Neoplasma *57*: 79-85, 2010.

19 Ding X, Xu Q, Liu F, Zhou P, Gu Y, Zeng J, An J, Dai W and Li X: Hematoporphyrin monomethyl ether photodynamic damage on HeLa cells by means of reactive oxygen species production and cytosolic free calcium concentration elevation. Cancer Lett *216*: 43-54, 2004.

20 Li B, Chen Z, Liu L, Huang Z andXie S: Differences in sensitivity to HMME-mediated photodynamic therapy between EBV+ C666-1 and EBV- CNE2 cells. Photodiagnosis Photodyn Ther *7*: 204-209, 2010.

21 Gupta S, Dwarakanath BS, Muralidhar K and Jain V: Cellular uptake, localization and photodynamic effects of haematoporphyrin derivative in human glioma and squamous carcinoma cell lines. J Photochem Photobiol B *69*: 107-120, 2003.

22 Mikes J, Kleban J, Sackova V, Horvath V, Jamborova E, Vaculova A, Kozubik A, Hofmanova J and Fedorocko P: Necrosis predominates in the cell death of human colon adenocarcinoma HT-29 cells treated under variable conditions of photodynamic therapy with hypericin. Photochem Photobiol Sci *6*: 758-766, 2007.

23 Osaki T, Takagi S, Hoshino Y, Okumura M and Fujinaga T: Intracellular localization and concentration as well as photodynamic effects of benzoporphyrin derivative monoacid ring A in four types of rodent tumor cells. Cancer Lett *243*: 281-292, 2006.

24 Song K, Kong B, Qu X, Li L and Yang Q: Phototoxicity of Hemoporfin to ovarian cancer. Biochem Biophys Res Commun *337*: 127-132, 2005.

25 Wei Y, Kong B, Song K, Qu X, Jin Q and Yang Q: Involvement of mitochondria-caspase pathway in Hemoporfin-mediated cell death. Photochem Photobiol *83*: 1319-1324, 2007.

Received July 19, 2011
Revised August 8, 2011
Accepted August 9, 2011